Molecular Dynamics Simulation of Polymer Nanoparticle Collisions: Internal Reorganization and Translation−Vibration Coupling

B. C. Hathorn,*,† B. G. Sumpter,† D. W. Noid,† and M. D. Barnes‡

Computer Science and Mathematics Division, Oak Ridge National Laboratory, Oak Ridge, Tennessee 37831, and Chemical and Analytical Sciences Division, Oak Ridge National Laboratory, Oak Ridge, Tennessee 37831

Received July 6, 2001; Revised Manuscript Received November 5, 2001

ABSTRACT: The dynamics of collisions of polymer particles is discussed in some detail. Particular attention is paid to the development of inter- and intraparticle potentials and to the apparent oscillatory behavior in the center-of-mass separation coordinate for the two particles. It is shown that the center-of-mass separation coordinate is closely coupled to the other vibrational coordinates and that vibrations in the center-of-mass separation are coupled to the intraparticle reorganization. The high degree of coupling between the translational and vibrational motions leads to a large degree of translational to vibrational energy exchange and leads to a strong propensity of particle collisions to result in attachment and particle dimer formation.

I. Introduction

There has been much development on the field of experimental production and investigation of monodisperse polymer nanoparticles[1−9] and accompanying theoretical simulations and investigations of their properties.[10−21] Recently, it has been observed that it is possible to construct well-defined and long-lived macrostructures composed of sequentially attached particles using a linear quadrapole as a particle positioning tool[27] (Figure 1). Physical measurements demonstrate that the polymer nanoparticles retain much of their internal structure in the larger assembly. In essence, the larger superstructure is composed of a collection of polymer beads, each of which is itself a collection of smaller monomer units. However, the mechanism of attachment and binding is unclear.

Phenomenological and atomistic studies of particle coalescence and annealing has shown that if collision times are shorter than the coalescence times, collisions of particles will result in the growth of single large particles, rather than a collection of smaller attached particles.[28−37] However, polymer chains of sufficient length may not migrate freely between the colliding particles, as do atoms in silica particles, inhibiting the reorganization of the collision cluster and leading to long coalescence times.

The picture of sequential attachment suggests the possibility to understand the particle attachment process and the superstructure of the larger system in terms of effective forces between the smaller spherical particles from which it is composed. Application of this approach will greatly simplify calculations on the system, by replacing the $3(N \times M)$ degrees of freedom for N polymer particles with M monomers each, to a problem of $3N$ degrees of freedom. In the reduced dimensionality framework, the superparticle can be construed as a collection of smaller bodies, each made up of a collection of monomer units. This approach is indicated when there is some average structure which can be used to represent the particles without resorting to computation of the exact details of the internal structure.

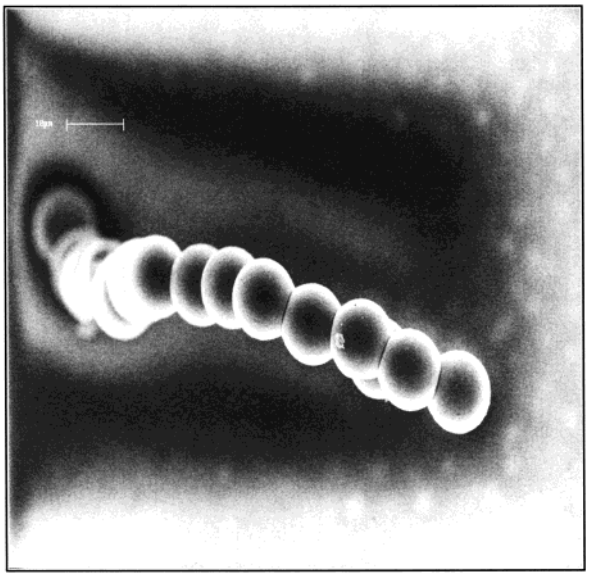

Figure 1. Experimental picture of a chain of polymer nanospheres. Particles were prepared using the techniques in ref 27.

In the present article, we present the first simulations of collisions of large-scale polymer nanoparticles. The particles employed in the present simulations are different from other recently studied particle collisions[28] not only in their size (the present particles are an order of magnitude larger than previously studied solid-state particles) but also in the transport properties of the monomer subunits. The strong bonds between sequential monomers in the polymer chains serves to substantially restrict migratory transport of the individual units. The restricted chain transport serves to preserve the polymer particles as distinct entities when in near contact. The simulation methodology employed also

† Computer Science and Mathematics Division.
‡ Chemical and Analytical Sciences Division.

10.1021/ma011172z CCC: $22.00 © 2002 American Chemical Society
Published on Web 01/03/2002

differs from much of the polymer literature, which focuses on Monte Carlo algorithms, lattice models, Brownian dynamics, renormalization, and coarse graining models, or is restricted to molecular dynamics on polymer systems of relatively short chain lengths and sizes.[22−26]

The approach in the present paper is to investigate the behavior of the internal structure of the particles with a generalized average behavior near the equilibrium value of the external separation of the centers of mass of the polymer particles. The small oscillations near this equilibrium value are then characterized by effective vibrational frequencies representing the interaction between the particles making up the larger agglomerate.

In section II we describe the procedures used in the simulation of the collisions. In section III we describe the results of our calculations for a number of initial conditions.

II. Simulation Methodology

For the purposes of the present study, we have examined motions and interaction forces between individual polymer particles both before and after interactions take place. The details of the geometric statement function approach employed are described more fully elsewhere.[38]

Polymer particles have been treated with a molecular dynamics approach,[39,40] integrating Hamilton's equations of motion in time,

$$\frac{\mathrm{d}q_i}{\mathrm{d}t} = \frac{\partial H}{\partial p_i} \tag{1}$$

$$-\frac{\mathrm{d}p_i}{\mathrm{d}t} = \frac{\partial H}{\partial q_i} \tag{2}$$

where H is the Hamiltonian of the system and the q_i and p_i represent the coordinates and their conjugate momenta. In the present case, we have treated coordinates and momenta in the Cartesian frame, where the total kinetic energy is diagonal. Integration of the equations of motion was accomplished by use of novel symplectic integrators developed in our laboratory.[41]

As a simplification we have collapsed the CH_2 and CH_3 units of the polyethylene chain into a single monomer of mass 14.5 amu. By neglecting the internal structure of these groups, the number of coordinates and thus the number of equation of motion for the system are greatly reduced. The model has been shown to be useful to study the low-temperature behavior of the system where the effects of the hydrogens have little effect on the heat capacity and entropy of the system.[42]

The Hamiltonian for the system is specified as[9,42]

$$H = T + \sum V_{2b} + \sum V_{3b} + \sum V_{4b} + \sum V_{nb} \tag{3}$$

where T is the kinetic energy component, expressed in terms of Cartesian coordinates, and the terms V_{2b}, V_{3b}, and V_{4b} represent the two-, three-, and four-body terms for monomer units in an individual polymer strand, and V_{nb} is the nonbonded interaction between individual monomer units separated by four or more monomer units along the chain and within a spherical cutoff of 10 Å. The functional forms of the potentials are given by[42−46]

Table 1. Potential Parameters for Polyethylene Particle Systems

two-body bonded constants[a]	four-body bonded constants[a]
$D = 334.72$ kJ/mol	$a = -18.4096$ kJ/mol
$r_e = 1.53$ Å	$b = 26.78$ kJ/mol
$\alpha = 199$ Å^{-1}	two-body nonbonded constants[a]
three-body bonded constants[b]	$\epsilon = 0.4937$ kJ/mol
$\gamma = 130.122$ kJ/mol	$\sigma = 4.335$ Å
$\theta_e = 113°$	

[a] References 45 and 46. [b] References 43 and 44.

$$V_{2b} = D\{1 - \exp[-\alpha(r_{ij} - r_e)]\} \tag{4}$$

$$V_{3b} = {}^1/_2\gamma(\cos\theta - \cos\theta_e)^2 \tag{5}$$

$$V_{4b} = 8.77 + a\cos\tau + b\cos^3\tau \tag{6}$$

$$V_{nb} = 4\epsilon\left[\left(\frac{\sigma}{r_{ij}}\right)^{12} - \left(\frac{\sigma}{r_{ij}}\right)^{6}\right] \tag{7}$$

with the values of the constant terms given in Table 1. The distances between the various monomer units, r_{ij}, are given by the standard Cartesian relation

$$r_{ij} = \sqrt{(x_i - x_j)^2 + (y_i - y_j)^2 + (z_i - z_j)^2} \tag{8}$$

In the present case, initial conditions for the trajectories comprised the coordinates of individual polymer particles, which had previously been obtained by an annealing,[14] with momenta chosen randomly in the radial coordinate so as not to excite internal angular momentum. (The contributions of angular momentum in the system will be discussed in a subsequent communication.) The randomly chosen momenta were rescaled so as to produce the appropriate temperature for the simulation,

$$\sum_i \frac{1}{2m_i}p_i^2 = \frac{3}{2}Nk_BT \tag{9}$$

The thermalized particles were then offset in the z-coordinate and given an initial relative velocity in the z-coordinate so as to produce a collinear collision. The initial offset was chosen so as to give at least 1 ps of time for the particles thermally equilibrate before coming within the maximum range of forces with the other particle (in the present case, 10 Å) (Figure 2).

A number of statistics were followed during the course of the trajectories, including inter- and intraparticle potential energies, configurational positions of the particles, and the separation of the centers of mass of the particles.

III. Results and Discussion

Initial conditions for polymer particles were obtained from previously annealed particles of approximately 5.6 nm in diameter.[14] For the purpose of generating interaction potentials between two polymer particles, particles were placed in near contact (with a center-of-mass separation of approximately 60 Å, an internal temperature of 5 K, and varying amounts of relative translational energy). The simulation was allowed to run for a minimum of 160 ps, at which point the particles were

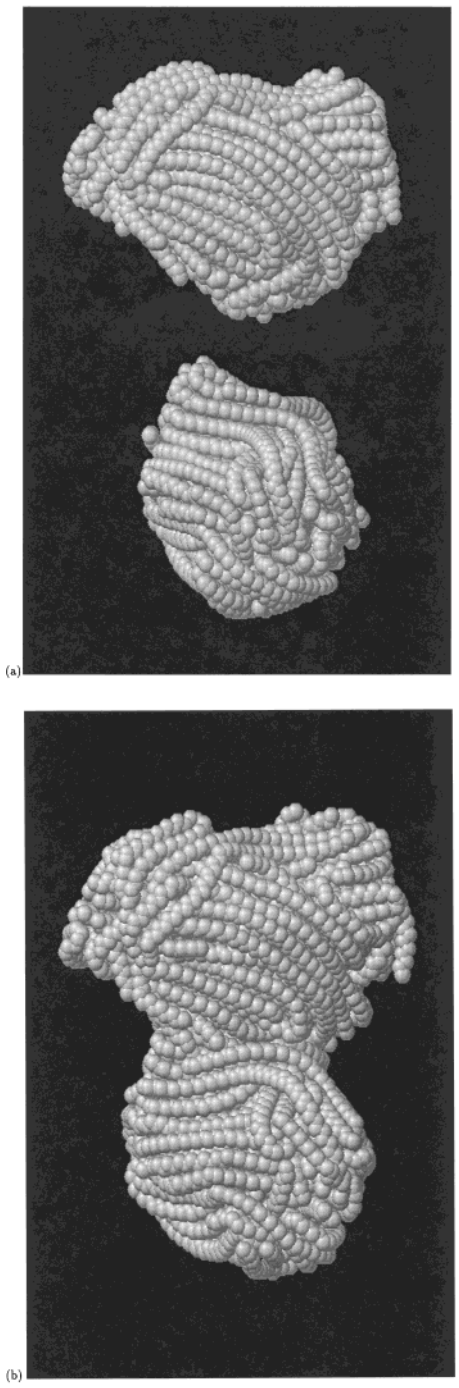

Figure 2. (a) Initial positions of two particles composed of 30 chains of 100 monomer units. (b) Positions of polymer particles composed of 30 chains of 100 monomer units after 80 ps. Particle collisions took place with an initial relative velocity of 1 Å/ps.

observed to have undergone substantial deformation and annealed into a stable configuration, with apparent small oscillations about the equilibrium center-of-mass separation (Figure 3).

A measure of the potential between the two particles is taken as the sum over the nonbonded (Lennard-Jones) forces involving monomer units in different particles. An illustration of the time dependence of the interparticle interaction, for two particles of 30 chains of 100 monomers with an initial temperature of 5 K, as the particles relax is shown in Figure 4. The upper curve represents the interactions of the two particles in the

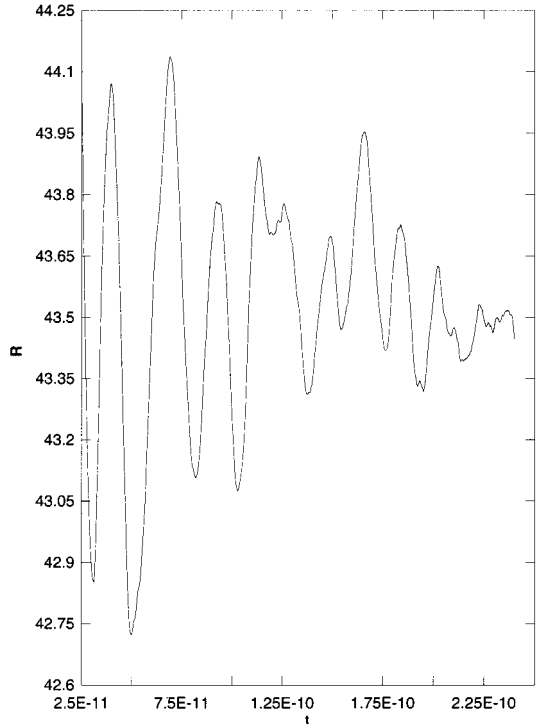

Figure 3. Time dependence of center-of-mass separation for the two particles. Particles had 30 chains of 100 monomer units and an internal temperature of 5 K and initial relative velocity of 1 Å/ps.

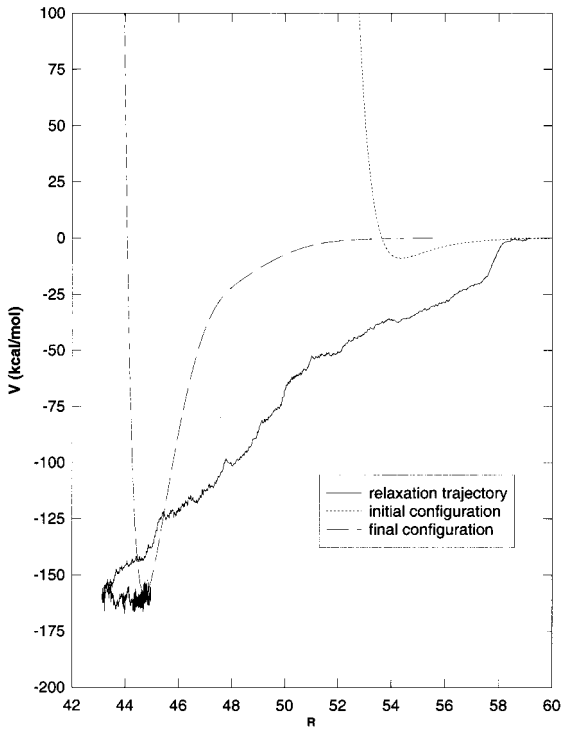

Figure 4. Interparticle interaction potentials for particles in initial and final configurations and the interaction potential during the relaxation process.

initial configuration when no deformation is permitted. The curve with the more stable minimum represents the potential at the final configuration, again, with no particle deformation permitted. The final line represents the potential between the two particles during the relaxation process. It is apparent that the particles gain significant relative translational energy and then re-

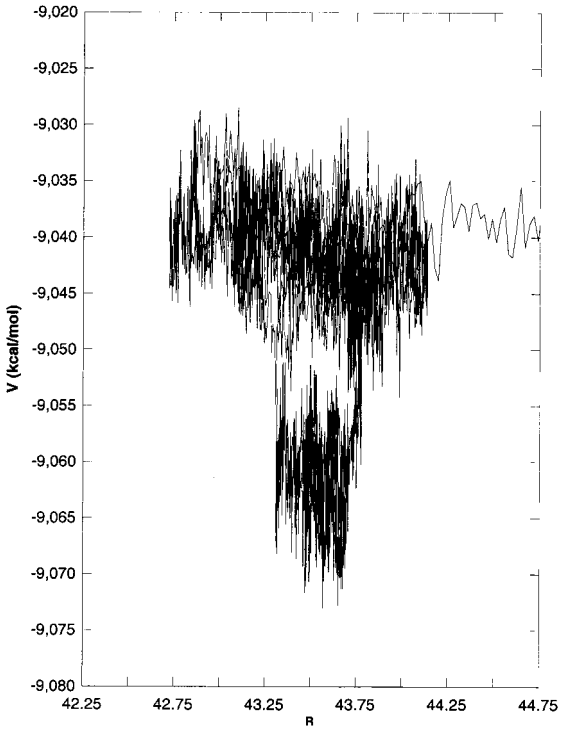

Figure 5. Intraparticle interaction potentials for particles during the relaxation process. Initial particles have 30 chains of 100 monomer units, an internal temperature of 5 K, and an initial relative velocity of 1 Å/ps. Restricted to the region surrounding the final configurations.

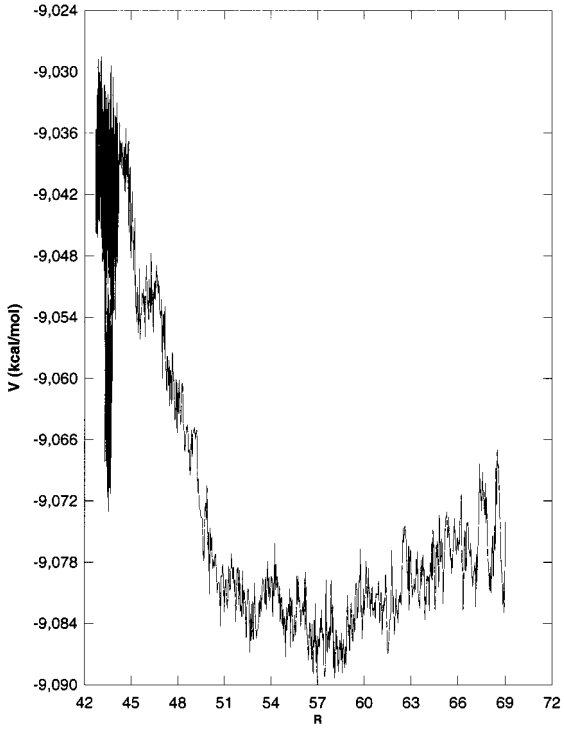

Figure 6. Intraparticle interaction potentials for particles during the relaxation process. Initial particles have 30 chains of 100 monomer units, an internal temperature of 5 K, and an initial relative velocity of 1 Å/ps. Identical to Figure 5, with the exception that the complete trajectory is shown.

bound from a hard core at a center-of-mass separation of approximately 43 Å, finally equilibrating at a separation of approximately 44.5 Å.

Our calculations show that there is a strong tendency of molecules to undergo deformation when in close proximity. The result of this deformation is to allow the center-of-mass separation of the particles to achieve distances substantially closer than would be allowed by undistorted particles, where the spatial constraints would require the particles to overlap in space, inevitably inducing steric conflicts in the positions of the monomer units. In Figure 4 we observe that the undeformed particles would have significant barriers to approach closer than approximately 54 Å, but in the simulated trajectory the ultimate equilibrium position occurs at a distance of approximately 45 Å. The close approach to a distance of approximately 43 Å does not tell the whole story, since such a close approach has nearly the same interparticle energy as the ultimate equilibrium at 45 Å, but at this point the intraparticle energy is higher (Figure 5) and at somewhat longer distances this potential term can be reduced, ultimately driving the separation to its final distance. Thus, the vibrational motion in the center-of-mass separation is largely characterized by the potential for the intraparticle reorganization, rather than by the interparticle potential, as one might initially suspect.

Ultimately, the interaction energy of the particles can be understood in terms the competition between the two terms: the optimization of the "volume" of a particle with respect to its surface area, and the interparticle reorganization energy, with the total energy being the sum of both terms. The minimization of the surface area with respect to the volume is hindered by the failure of long polymer chains in the particle to undergo large-scale migration due to the steric effects of entanglement. While it might be energetically favorable to reorganize the two (approximately) spherical initial particles into a new, larger (approximately) spherical particle, at low energies there is insufficient energy to overcome the barriers for such a global reorganization. Once a major reorganizational step has been accomplished, however, it is essentially irreversible. Such an effect can be illustrated in Figure 5. There are two distinct vibrations, one with an average internal particle potential of approximately −9040 kcal/mol and the other with an average potential of approximately −9060 kcal/mol. The latter vibration having a somewhat smaller amplitude of center-of-mass vibration. The two vibrations have similar vibrational frequencies, however, with the transition between the two oscillations occurring at approximately 1.2×10^{-10} s in Figure 3.

The contribution of the optimization of the surface area with respect to the volume can be observed in the full trajectory of the internal potential of the particle (Figure 6). We find that the final trajectory position is not near the location of the minimum of the intraparticle potential; however, the increased potential at this configuration is made up in the reduction in the interparticle potential terms, resulting in a lower total potential, as in Figure 7.

It is interesting to note that, despite the complexity of the potential, and the fact that it is dependent on the configuration of the superparticles, there are some general trends that are true. The final equilibrium distances for the oscillations and the vibrational periods can be estimated from graphs similar to Figure 3. The frequencies obtained in this matter will not be true vibrational frequencies for center-of-mass separation normal mode, as it is clear that such a vibration must

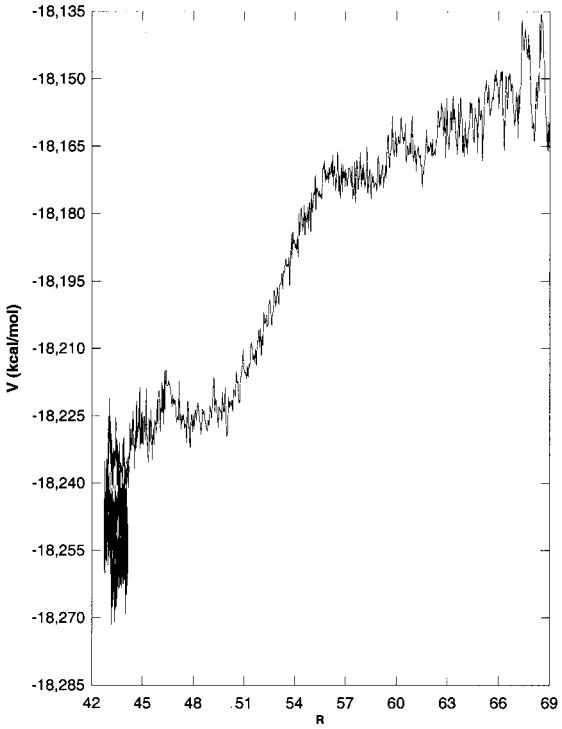

Figure 7. Total potential for particles during the relaxation process. Initial particles have 30 chains of 100 monomer units, an internal temperature of 5 K, and an initial relative velocity of 1 Å/ps.

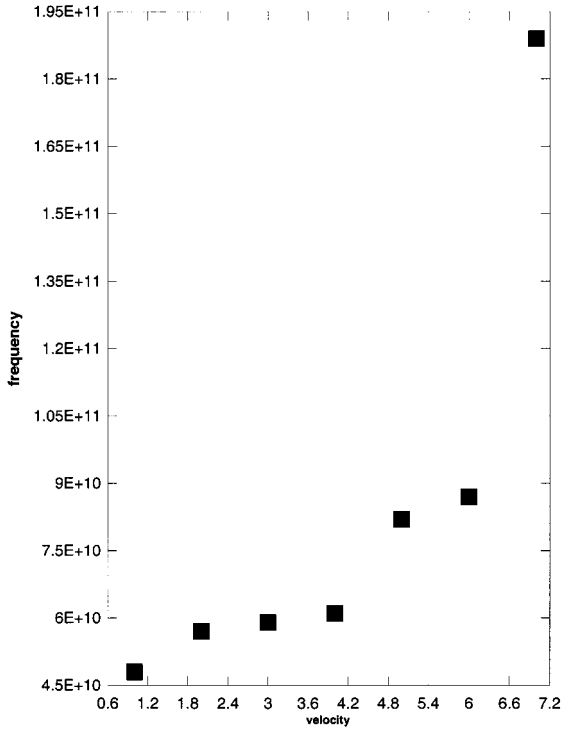

Figure 8. Equilibrium center-of-mass separation as a function of initial relative translational velocity. Polymer particles are 30 chains of 100 monomer units with an initial internal temperature of 5 K.

be coupled to other motions, as is evidenced by the vibrational damping. Nonetheless, there is a certain trend in the periods of vibration and equilibrium vibrational distance as a function of initial relative velocity which is evident. It is very interesting, as was pointed out in the discussion of the transition between the two structures in Figure 3 at 1.2×10^{-10} s, that the vibrational frequency seems to be more dependent on the initial velocity than on the exact configuration of the ensuing complex. At energies where the collision results in entanglement and gross reorganization of the particles, the equilibrium center of mass separation is reduced, and the corresponding harmonic curvature of the coordinate is increased, leading to correspondingly higher vibrational frequencies (Figures 8 and 9).

Force constants and vibrational frequencies for the effective center-of-mass vibrations can be determined by two different methods. Presuming the motion to be primarily along the coordinate of the center-of-mass separation, one can apply the second derivative of the potential with respect to variation of the center-of-mass separation distance at the relaxed equilibrium configuration. The vibrational frequencies obtained in this manner for the harmonic multibody potential are higher than one might expect, given the large reduced mass of the system. Such a high effective curvature of the potential surface arises from the large number of terms in the vicinity of the equilibrium position, effectively proportional to the surface contact area of the pair after relaxation. It is clearly possible, however, to circumvent the steep potential in this region by distortion of other normal coordinates of the molecular spheres. Such a pathway is followed during the collision of the particles (in Figure 4), and such reorganizational motion is sufficiently fast so as to allow the collision to follow the lower energy pathway.

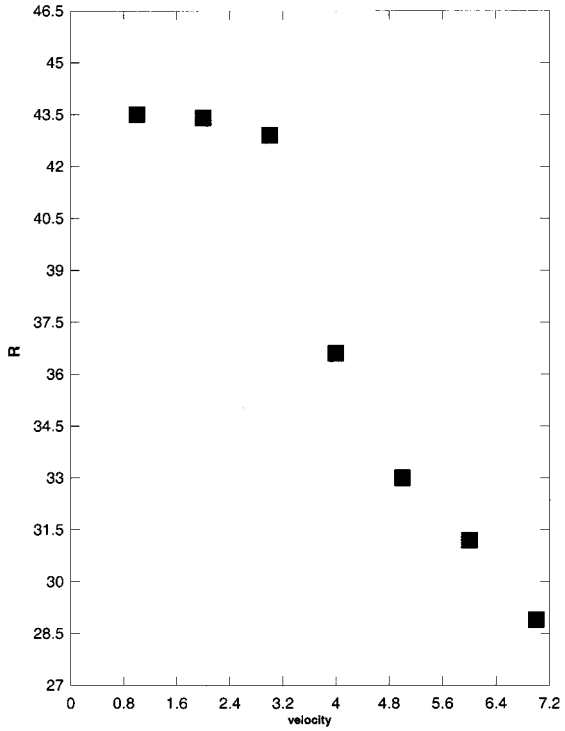

Figure 9. Center-of-mass separation vibrational frequency as a function of initial relative translational velocity. Polymer particles are 30 chains of 100 monomemer units with an initial internal temperature of 5 K.

The actual frequencies for the pseudo-vibrational motion in the center-of-mass separation coordinate can be deduced by analysis of the oscillatory behavior in the center-of-mass separation, as in Figure 3. The vibrational period is estimated from the peak-to-peak recurrence times over several vibrational periods and is seen

to produce vibrational frequencies substantially smaller than those that are derived by an expansion of the potential near the minimum. The disparity can be construed as evidence that the motion of the particle is poorly represented by a normal coordinate resembling the pure center-of-mass separation, with the particle configurations fixed. During the oscillation period there must be substantial reorganization of the particles. The strong coupling of the internal structure of the particles to the overall motion with respect to the center-of-mass separation of the particles likely precludes any very accurate multibody potential. One can, however, obtain a very approximate, average harmonic potential, based on the oscillations after the equilibration of the particles.

The vibrational frequencies show a clear dependence on the velocity of the initial impact, with higher velocities allowing for a deeper interparticle penetration and a shorter equilibrium center-of-mass separation. At the same time, greater "entanglement" of the polymer chains in the particles for higher velocity collisions leads to obstructions to a dissociation along the center-of-mass coordinate, with collisions with greater than approximately 4 Å/ps having a barrier in the center-of-mass separation coordinate to redissociation. The entanglement is also evidenced by the dramatic shift in the distance of the equilibrated center of mass. In polymers showing entanglement, the center-of-mass separation at the equilibrium is decreased by approximately 10 Å, indicating significantly more interpenetration of the particles.

The complex reaction pathway poses an interesting question in the phenomenon of particle collisions. The minimum-energy pathway is clearly very complex, involving numerous collective motions of the interacting polymer chains. As a result, during the collision process, much of the available kinetic energy is conferred to vibrations in these modes and is thus not available for localization into a true dissociative reaction coordinate. As a result, the collisions of the polymer particles appear to stick uniformly until very high energies. We shall discuss this phenomenon in detail in a subsequent communication.

In comparison to the experimental results, we note that the polyethylene particles in the present calculation show propensity to substantially more internal reorganization than the experimental particles, which demonstrate structural stability during the collision process. The experimental polymer spheres are, however, substantially larger than those in the present simulation (on the order of microns rather than nanometers), and the displacement of a polymer chain by a few nanometers will not grossly affect the shape of the particle. In addition, the composition of the experimental particles is slightly different than the present polyethylene, the particles being composed of a composite of polymers which are more rigid than polyethylene and some which are less apt to keep their structure. As a result, the particles in the experimental system are likely much more rigid than those in the present calculation.

Acknowledgment. We thank the reviewers for their insightful comments which helped to prepare the manuscript for publication. In particular, we thank them for pointing out ref 22, which was published shortly after this work was submitted. This work was sponsored by the Division of Computer Science and Mathematics and the Division of Materials Sciences, Office of Basic Energy Sciences, U.S. Department of Energy under Contract DE-AC05-00OR22725 with UT-Battelle at Oak Ridge National Laboratory (ORNL), using resources of the Center for Computational Sciences at Oak Ridge National Laboratory. B.C.H. has been supported by the Postdoctoral Research Associates Program administered jointly by ORNL and the Oak Ridge Institute for Science and Education.

References and Notes

(1) Kung, C.-Y.; Barnes, M.; Sumpter, B. G.; Noid, D. W.; Otaigbe, J. *Polym. Prepr.* **1998**, *39*, 610.
(2) Barnes, M. D.; Kung, C.-Y.; Sumpter, B. G.; Noid, D. W.; Otaigbe, J. *Opt. Lett.* **1999**, *24*, 121.
(3) Barnes, M. D.; Ng, K. C.; Fukui, K.; Sumpter, B. G.; Noid, D. W. *Mater. Today* **1999**, *2*, 25.
(4) Barnes, M. D.; Ng, K. C.; Fukui, K.; Sumpter, B. G.; Noid, D. W. *Macromolecules* **1999**, *32*, 7183.
(5) Ford, J. V.; Sumpter, B. G.; Noid, D. W.; Barnes, M. D. *Chem. Phys. Lett.* **2000**, *316*, 181.
(6) Ford, J. V.; Sumpter, B. G.; Noid, D. W.; M. D. Barnes, M. D. *J. Phys. Chem. B* **2000**, *104*, 495.
(7) Ford, J. V.; Sumpter, B. G.; Noid, D. W.; Barnes, M. D. *Polymer* **2000**, *41*, 8075.
(8) Ford, J. V.; Sumpter, B. G.; Noid, D. W.; Barnes, M. D.; Otaigbe, J. U. *Appl. Phys. Lett.* **2000**, *77*, 2515.
(9) Otaigbe, J.; Barnes, M.; Fukui, K.; Sumpter, B. G.; Noid, D. W. *Adv. Polym. Sci.* **2001**, *154*, 1.
(10) Fukui, K.; Sumpter, B. G.; Barnes, M.; Noid, D. W.; Otaigbe, J. *Polym. Prepr.* **1998**, *39*, 612.
(11) Fukui, K.; Sumpter, B. G.; Barnes, M. D.; Noid, D. W.; Otaigbe, J. *Macromol. Theory Simul.* **1999**, *8*, 38.
(12) Fukui, K.; Sumpter, B. G.; Runge, K.; Kung, C. Y.; Barnes, M.; Noid, D. W. *Chem. Phys.* **1999**, *244*, 339.
(13) Fukui, K.; Sumpter, B. G.; Barnes, M. D.; Noid, D. W. *Comput. Theor. Polym. Sci.* **1999**, *9*, 245.
(14) Fukui, K.; Sumpter, B. G.; Barnes, M. D.; Noid, D. W. *Polym. J.* **1999**, *31*, 664.
(15) Noid, D. W.; Fukui, K.; Sumpter, B. G.; Yang, C.; Tuzun, R. *Chem. Phys. Lett.* **2000**, *316*, 285.
(16) Fukui, K.; Noid, D. W.; Sumpter, B. G.; Yang, C.; Tuzun, R. *J. Phys. Chem. B* **2000**, *104*, 526.
(17) Sumpter, B. G.; Barnes, M. D.; Fukui, K.; Noid, D. W. *Mater. Today* **2000**, *2*, 3.
(18) Fukui, K.; Sumpter, B. G.; Yang, C.; Noid, D. W.; Tuzun, R. E. *J. Polym. Sci., Polym. Phys.* **2000**, *38*, 1812.
(19) Fukui, K.; Sumpter, B. G.; Barnes, M. D.; Noid, D. W. *Macromolecules* **2000**, *33*, 5982.
(20) Sumpter, B. G.; Fukui, K.; Barnes, M. D.; Noid, D. W. In *Computational Studies, Nanotechnology, and Solution Thermodynamics of Polymer Systems*; Kluwer Academic/Plenum Publishers: Dordrecht, 2001.
(21) Fukui, K.; Sumpter, B. G.; Yang, C.; Noid, D. W.; Tuzun, R. E. *Comput. Theor. Polym. Sci.* **2001**, *11*, 191.
(22) Vao-soongern, V.; Ozisik, R.; Mattice, W. L. *Macromol. Theory Simul.* **2001**, *10*, 553.
(23) Doruker, P.; Mattice, W. L. *Macromol. Theory Simul.* **2001**, *10*, 363.
(24) Milchev, A.; Binder, K. *J. Chem. Phys.* **2001**, *114*, 8610.
(25) Kumar, S.; Larson, R. G. *J. Chem. Phys.* **2001**, *114*, 6937.
(26) Kumar, S. *Physica A* **2001**, *292*, 422.
(27) (a) Barnes, M. D.; Mahurin, S.; Mehta, A.; Sumpter, B. G.; Noid, D. W. *Phys. Rev. Lett.*, in press. (b) Mahurin, S. M.; Mehta, A.; Hathorn, B. C.; Sumpter, B. G.; Noid, D. W.; Runge, K.; Barnes, M. D. *Opt. Lett.*, in press.
(28) Zachariah, M. R.; Carrier, M. J. *J. Aerosol Sci.* **1999**, *30*, 1139 and references therein.
(29) German, R. M. *Sintering Theory and Practice*; Wiley: New York, 1996, and references therein.
(30) Kingery, W. D.; Berg, M. *J. Appl. Phys.* **1955**, *26*, 1205.
(31) Nichols, F. A.; Mullins, W. W. *J. Appl. Phys.* **1965**, *36*, 1826.
(32) Nichols, F. A. *J. Appl. Phys.* **1966**, *37*, 2805.
(33) Lehtinen, K. E. J.; Zachariah, M. R. *Phys. Rev. B* **2001**, *63*, 205402.
(34) Zhu, H. L.; Averback, R. S. *Mater. Manufacturing Proc.* **1996**, *11*, 905.
(35) Zhu, H. L.; Averback, R. S. *Philos. Mag. Lett.* **1996**, *73*, 27.

(36) Blasiten-Barojas, E.; Zachariah, M. R. *Phys. Rev. B* **1992**, *45*, 4403.
(37) Gay, J. G.; Berne, B. J. *J. Colloid Interface Sci.* **1986**, *109*, 90.
(38) Noid, D. W.; Sumpter, B. G.; Wunderlich, B.; Pfeffer, G. A. *J. Comput. Chem.* **1990**, *11*, 236.
(39) Hoover, W. G. *Annu. Rev. Phys. Chem.* **1983**, *34*, 103.
(40) Klein, M. L. *Annu. Rev. Phys. Chem.* **1985**, *36*, 525.
(41) Gray, S. K.; Noid, D. W.; Sumpter, B. G. *J. Chem. Phys.* **1994**, *101*, 4062.
(42) Sumpter, B. G.; Noid, D. W.; Wunderlich, B. *J. Chem. Phys.* **1990**, *93*, 6875.
(43) Weber, T. A. *J. Chem. Phys.* **1978**, *69*, 2347.
(44) Weber, T. A. *J. Chem. Phys.* **1979**, *70*, 4277.
(45) Sorensen, R. A.; Liam, W. B.; Boyd, R. H. *Macromolecules* **1988**, *21*, 194.
(46) Boyd, R. H. *J. Chem. Phys.* **1968**, *49*, 2574.

MA011172Z